# Temporal Theil scaling in diffusive trajectory time series

F. S. Abril [*] and C. J. Quimbay [†]
*Universidad Nacional de Colombia, Departamento de Física, 111321 Bogotá D.C., Colombia.*

(Received 12 November 2021; revised 7 April 2022; accepted 23 June 2022; published 15 July 2022)

Temporal fluctuation scaling (TFS) is a power-law relation between the variance ($\Xi$) and the mean ($\Upsilon$) which is present in cumulative time series. Taking into account that Theil index ($T$) can be assumed as a measure of dispersion and considering diffusive trajectory time series, we find a power-law relation between $T$ and $\Upsilon$ of the form $T \sim (1 - c\Upsilon)^{\beta}$, which we call temporal Theil scaling (TTS). Specifically, by analyzing data of volatility and absolute log-return for 24 nonstationary time series of financial markets, meteorology, and COVID-19 spread, we find that TTS is present in diffusive trajectory time series, while TFS is not present. Furthermore, we show that the power-law relation of TTS has a form that is similar to the relation between order parameter and temperature, which is found in the Ginzburg-Landau theory when the nontrivial critical points of an energy functional $\mathcal{F}_{\eta,\delta}$ containing arbitrary powers $\eta$ and $\delta$ of the order parameter are calculated.

DOI: 10.1103/PhysRevE.106.014117

## I. INTRODUCTION

Fluctuation scaling (FS) is a property that can be presented in a set of empirical data of complex systems in such a way that the variance ($\Xi$) of the data is related with the mean ($\Upsilon$) of the data through a power-law relation of the form $\Xi \sim \Upsilon^{\alpha}$, where the dispersion (fluctuation) of the data has been described in terms of $\Xi$ [1–3]. Since its discovery in 1938 by F. Smith [4], FS has had two approaches, spatial (ensemble fluctuation scaling) and temporal (temporal fluctuation scaling). In particular, temporal fluctuation scaling (TFS) has been observed in cumulative time series as an emergent property of complex systems from different branches of science [5–7]. For instance, in financial time series, it has been observed that by defining $\Upsilon$ and $\Xi$ with an optimal window size, the trend of the data can be characterized by a logarithmic behavior, where the value of $\alpha$ is not universal and does not depend on the market type [1,8–12]. Here it is worth noting that in the context of financial markets, TFS allows to characterize the type of market from its exponent $\alpha$ and its temporal evolution [1,8]. Also, TFS has been found in the spread of the COVID-19 pandemic around the world for the time series of cumulative daily confirmed cases and daily deaths [13]. However, it has not been investigated if TFS can be also observed in another kind of time series, specifically in diffusive trajectory time series [14]. Moreover, it has also not been investigated for the case of diffusive trajectory time series whether another quantity that can be used to measure dispersion of data is related with $\Upsilon$ through a power-law relation. However, the Theil index ($T$) is a measure of inequality introduced by the Dutch economist Henri Theil in terms of the entropy index [15]. Given that $T$ measures the inequality in empirical income distributions of a population [16], this inequality index exhibits the important property of decomposition because it can be calculated from the inequalities of the subgroups in which the population is partitioned [17]. Additionally, $T$ can be also used to characterize racial segregation [18]. Besides, $T$ can be seen as a measure of redundancy in the data or diversity [19–21]. Thus, for the case in which $T$ is normalized to the logarithm of the number of data, this index has a value 0 for maximum equality, while its value is 1 for maximum inequality. Likewise, the most popular measure of inequality of an income distribution in a population corresponds to the Gini index ($G$), which was introduced by the Italian sociologist Corrado Gini in 1912 [22]. Furthermore, analogous to the normalized $T$, the case $G = 0$ represents the maximum equality, while $G = 1$ represents the maximum inequality. In particular, for a parametric family of probability distributions, it has been shown that $G$ can be seen as a measure of dispersion because it can be written in terms of $\Xi$ [23]. Also, it has been shown that $T$ can be calculated in terms of $\Xi$ for the most important and popular parametric income distributions [24]. Indeed, it has been shown that the relation between $T$ and $\Xi$ depends on the type of probability distribution to which a data set fits [24]. Thus, in general, $T$ is related to $\Xi$ as suggested in Ref. [25], and in this form, $T$ can be seen as a measure of dispersion. It is worth mentioning that $T$ has been used in the context of econophysics to study the correlation of time series with different metrics and emphasizing that the latter transforms the time series into entropy time series (depending on the the time window size) [26]. Other econophysical applications of $T$ lie in the study of the distribution of income in countries [27], the understanding of equilibrium states of free market models [28], and the use of an entropic approach to understand the regional changes in the distribution of foreign aid [29]. Due to the existence of a power-law relation between $\Xi$ and $\Upsilon$ in cumulative time series (TFS) and also by the relation between $T$ and $\Xi$ for different probability distributions, the existence of a relation between $T$ and $\Upsilon$ should be expected. With this idea in mind, we find from the analysis of the empirical data that TFS does not exist in the diffusive

[*] fsabrilb@unal.edu.co.
[†] cjquimbayh@unal.edu.co.

 

trajectory time series for volatility and absolute log-return of the following 24 nonstationary time series of financial markets, meteorology and COVID-19 spread: in financial markets for stock indexes as Nikkei 225, S&P 500, DAX, MOEX, IBEX 35, NASDAQ, BOVESPA, COLCAP, CAC 40, AEX, and RTS; for currencies as Colombian peso-dollar (COP-USD), bitcoin-dollar (BTC-USD), euro-dollar (EUR-USD), pound sterling-dollar (GBP-USD), and dollar-yen (USD-JPY); for commodities as silver, gold, crude oil, and treasure yield of United States [30]; in meteorological systems for temperature and precipitation in Bogota, Colombia, and in the spread of a pandemic for daily cases and deaths of COVID-19 in the United States of America. Contrary to the last result, we find that a power-law relation between $T$ and $\Upsilon$ of the form $T \sim (1 - c\Upsilon)^{\beta}$ is present in diffusive trajectory time series for volatility and absolute log-return of the mentioned 24 nonstationary time series. Thus, we call to this new type of temporal scaling involving $T$ as temporal Theil scaling (TTS). Finally, we show that the power-law relation of TTS has a similar form to that obtained between the order parameter ($\psi$) and the temperature ($\theta$), in the form $\|\psi\| \sim (1 - d\theta)^{\gamma}$, as it is found in the context of the Ginzburg-Landau theory when the nontrivial critical points of an energy functional $\mathcal{F}_{\eta,\delta}$ containing arbitrary powers $\eta$ and $\delta$ of the order parameter $\psi$ are calculated. The structure of this work is the following: in Sec. II we develop the definitions of the diffusive trajectory time series which are necessary to be able to find the TTS, and additionally the global average error [GAE(%)] and $\chi^2$ test are also defined to have an estimate of the quality of the adjustments shown. In Sec. III, from the analysis of the data of volatility and absolute log-return of the 24 time series studied in this work, first we find that TFS does not exist in diffusive trajectory time series for volatility and absolute log-return, next we show from the analysis of the data that $T$ and $\Xi$ are not related by a functional relation, and finally we find the existence of an empirical power-law relation between $T$ and $\Upsilon$, that we call TTS. In Sec. IV, using the Ginzburg-Landau theory, we show that $\psi$ and $\theta$ satisfy a power-law relation at the critical temperature ($\theta_c$) which has the same form that the empirical power-law relation of the TTS. Finally, in Sec. V we present the conclusions and future directions of this work.

## II. DIFFUSIVE TRAJECTORY TIME SERIES

A time series corresponds to the realization of a discrete stochastic process $Y_t$ with $t \in \mathbb{N}$. The weak-sense stationarity or wide-sense stationarity of a discrete stochastic process $Y_t$ is defined as a random process which the mean $\mathbb{E}[Y_t]$ and autocovariance function $\mathbb{E}[(Y_{t_1} - \mathbb{E}[Y_{t_1}])(Y_{t_2} - \mathbb{E}[Y_{t_2}])] \equiv K_{YY}(t_1, t_2)$, does not vary concerning time [31], that is

$$\mathbb{E}[Y_t] = \mathbb{E}[Y_{t+\tau}], \text{ for all } \tau \in \mathbb{N}, \tag{1}$$

$$K_{YY}(t_1, t_2) = K_{YY}(t_1 - t_2, 0), \text{ for all } t_1, t_2 \in \mathbb{N}, \tag{2}$$

$$\mathbb{E}\left[|Y_t|^2\right] < \infty, \text{ for all } t \in \mathbb{N}. \tag{3}$$

A time series is nonstationary if the above definition is not satisfied. Henceforth, it is assumed that the time series are nonstationary and for simplicity, from now on we will refer to time series as nonstationary time series. It is worth noting that Eq. (3) indicates that the variance of the time series is a finite number. For the study of the data of the 24 nonstationary time series that we consider in this work, two time series are defined with the data value $S_i$ given by the volatility (LV) and absolute log-return (LA), which correspond [9,32,33]

$$\mathrm{LV}_i = \frac{1}{\max_{1 \leqslant k \leqslant N} |\mathrm{LR}_k|} \sqrt{\left| \frac{\mathrm{LR}_i - \mathbb{E}[\mathrm{LR}]}{\sigma(\mathrm{LR})} \right|}, \tag{4}$$

$$\mathrm{LA}_i = |\mathrm{LR}_i|, \tag{5}$$

respectively, where $\mathrm{LR}_i$ is the log-return given by

$$\mathrm{LR}_i = \ln(S_{i+1}) - \ln(S_i). \tag{6}$$

The subindex refers to the time, $N$ is the total number of data of the time series, $\mathbb{E}[\cdot]$ is the expectation value, and $\sigma(\cdot)$ is the standard deviation. It is worth mentioning that in practical terms, Eq. (6) defines the time series of log-returns, which is distributed as a truncated Levy distribution [32,33], but our interest is focused on the time series of absolute log-return and volatility, which have the property of being positive definite. In addition, due to the structure of the temporal scaling that is proposed below with $T$ that involves the maximum [see Eq. (10)], it is useful to define the time series of volatility with the maximum. Then, each of these two time series (volatility and absolute log-return), is associated with a new time series through the diffusion algorithm exposed in Ref. [14], and defined by

$$x_{\mathrm{TS}}^{(s)}(t) = \sum_{j=1}^{t} \mathrm{TS}_{j+s}, \tag{7}$$

with $s = 0, 1, ..., N - t$ and $\mathrm{TS} = \mathrm{LV},\ \mathrm{LA}$. Equation (7) is known as the diffusive trajectory time series [14] and defines at each time step a subseries of $N - t + 1$ data, such that for $t = 1$ it corresponds to the original time series, for $t = 2$ it corresponds to the subseries obtained by adding two successive terms in the original series, and so on until $t = N$, where the subseries of a single piece of data is obtained whose value is the sum of all the terms of the original time series. Thus, a time step is defined in this context as the realization of the diffusive trajectory $x_{\mathrm{TS}}^{(s)}(t)$ of $N - t + 1$ data obtained from a successive sum of terms of the original time series TS. Finally, in this last time series $x_{\mathrm{TS}}^{(s)}(t)$, the mean $\Upsilon(t)$ and the variance $\Xi(t)$ are taken in each time step $t$, that is, the $N - t + 1$ data of the time subseries $x_{\mathrm{TS}}^{(s)}(t)$ are taken in the time step $t$, and from these the mean and the variance are calculated on the sample of $N - t + 1$ data. Taking into account that TFS is satisfied for the case of cumulative time series, we show that a power-law relation between $\Upsilon(t)$ and $\Xi(t)$ of the form

$$\Xi(t) = K|\Upsilon(t)|^{\alpha}, \tag{8}$$

where $K$ represents the TFS constant and $\alpha$ represents the TFS exponent, does not exist for the case of diffusive trajectory time series. Precisely, we show in the next section, that TFS is not present in none of the cases, for the 24 time series considered in this work. It is worth mentioning that Eq. (8) is exactly the power-law relation of the TFS, which is present for cumulative time series [1–3,9]. Now, since we

TABLE I. Start date and end date for the time series of the Nikkei 225, S&P 500, DAX, MOEX, IBEX 35, NASDAQ, BOVESPA, COLCAP, CAC 40, AEX, and RTS stock indexes, the Colombian peso-dollar (COP-USD), bitcoin-dollar (BTC-USD), euro-dollar (EUR-USD), pound sterling-dollar (GBP-USD), dollar-yen (USD-JPY) currencies, the silver, gold, crude oil commodities, the treasure yield of the United States, the temperature and precipitation in Bogota, Colombia, and the daily cases and deaths of COVID-19 in the United States.

| Time Series | Start date | End date |
|---|---|---|
| Nikkei 225 | 5/01/1965 | 10/03/2022 |
| S&P 500 | 4/01/2006 | 10/03/2022 |
| DAX | 30/12/1987 | 10/03/2022 |
| MOEX | 5/03/2013 | 10/03/2022 |
| IBEX 35 | 12/07/1993 | 10/03/2022 |
| NASDAQ | 5/02/1971 | 10/03/2022 |
| BOVESPA | 27/04/1993 | 10/03/2022 |
| COLCAP | 17/01/2008 | 10/03/2022 |
| CAC 40 | 1/03/1990 | 10/03/2022 |
| AEX | 12/10/1992 | 10/03/2022 |
| RTS | 4/09/1995 | 10/03/2022 |
| USD-COP | 9/11/1989 | 10/03/2022 |
| BTC-USD | 17/09/2014 | 10/03/2022 |
| EUR-USD | 1/12/2003 | 10/03/2022 |
| GBP-USD | 1/12/2003 | 10/03/2022 |
| USD-JPY | 30/10/1996 | 10/03/2022 |
| Silver | 30/08/2000 | 15/04/2021 |
| Gold | 30/08/2000 | 15/04/2021 |
| Crude Oil | 23/08/2000 | 15/04/2021 |
| Treasure Yield U.S. | 2/01/1962 | 10/03/2022 |
| Bogota Temperature | 1/03/2010 | 12/04/2021 |
| Bogota precipitation | 4/03/2010 | 25/09/2020 |
| Covid Cases USA | 21/01/2020 | 26/10/2021 |
| Covid Deaths USA | 29/02/2020 | 26/10/2021 |

want to study precisely the relation between $\Upsilon$ and $T$ for the diffusive trajectory time series, the Theil index is defined as [24]

$$T(t) = -\sum_k \frac{x_{\mathrm{TS}}^{(k)}(t)}{\bar{x}(t)M} \ln\left[\frac{x_{\mathrm{TS}}^{(k)}(t)}{\bar{x}(t)M}\right], \tag{9}$$

where $x_{\mathrm{TS}}^{(k)}(t)$ is the $k$th value of the diffusive trajectory at time $t$, $\bar{x}(t)$ is the mean of the diffusive trajectory at time $t$, and $M = N - t + 1$ is the total number of data in the diffusive trajectory at time $t$. From the analysis of data, we show in the next section that the data of volatility and absolute log-return of the 24 time series studied in this work satisfy the following empirical power-law relation

$$\frac{T(t)}{T(1)} = K_1 \left|1 - \frac{\Upsilon(t)}{\Upsilon_M}\right|^{\beta}, \tag{10}$$

where $\Upsilon_M = \max\{\Upsilon(j) | 1 \leqslant j \leqslant N\}$, $T(1)$ is the maximum value of the Theil index throughout the different time steps taken which corresponds to the first time step ($t = 1$), $K_1$ is the TTS constant and $\beta$ is the TTS exponent. Thus, we call this power-law relation involving $T$ as temporal Theil scaling (TTS). Furthermore, to measure the quality of the fits shown in Sec. III, the global average error $\mathrm{GAE}_T(\%)$ and $\chi^2$ test [34] are used, and these are defined as

$$\mathrm{GAE}_T(\%) = \frac{1}{N}\sum_{j=1}^{N}, \frac{|M(j) - T(j)|}{|T(j)|} \times 100\%, \tag{11}$$

$$\chi_T^2 = \sum_{j=1}^{N}, \frac{|M(j) - T(j)|^2}{T(j)}, \tag{12}$$

respectively, where $M(j)$ is the normalized Theil index of empirical data for the $j$th diffusive trajectory, and $T(j)$ is the adjustment of the normalized Theil index obtained from Eq. (10). Specifically, given a time step $t$, we have the time subseries $x_{\mathrm{TS}}^{(s)}(t)$ of $N - t + 1$ data, which allows us to calculate $M(t)$ from Eq. (9), while $T(t)$ is estimated from the adjustment made using the Eq. (10).

## III. EMPIRICAL RELATIONS IN DIFFUSIVE TRAJECTORY TIME SERIES

Before starting this section, some important detail in the calculation of the diffusive trajectory time series is highlighted: 100 time steps are taken due to the high computation time required to calculate $T$ at each time step for multiple time series. In addition, for completeness reasons, the Table I is added that indicates the time periods taken for each of the time series. In this table we can observe the presence of time series associated to financial markets, meteorological systems and an epidemiological system.

### A. Relation between variance and mean

This subsection shows that TFS does not exist for the diffusive trajectory time series of volatility and absolute

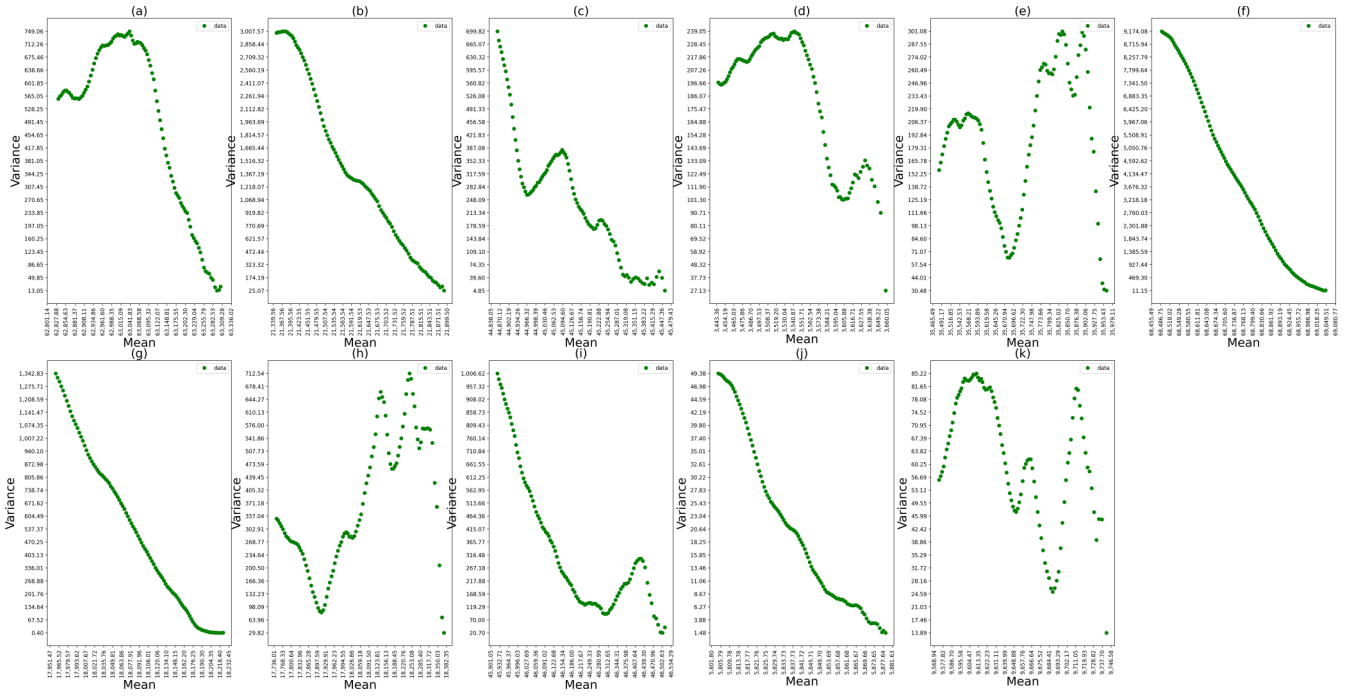


FIG. 1. Variance $\Xi$ as a function of the mean $\Upsilon$ for the diffusive trajectory time series of volatility of the: (a) Nikkei 225, (b) S&P 500, (c) DAX, (d) MOEX, (e) IBEX 35, (f) NASDAQ, (g) BOVESPA, (h) COLCAP, (i) CAC 40, (j) AEX, and (k) RTS stock indexes taking 100 time steps.

log-return for the following time series: Nikkei 225, S&P 500, DAX, MOEX, IBEX 35, NASDAQ, BOVESPA, COLCAP, CAC 40, AEX, and RTS stock indexes, the Colombian peso-dollar (COP-USD), bitcoin-dollar (BTC-USD), euro-dollar (EUR-USD), pound sterling-dollar (GBP-USD), dollar-yen (USD-JPY) currencies, the silver, gold, crude oil commodities, the treasure yield of the United States, the temperature and precipitation in Bogota, Colombia, and the daily cases and deaths of COVID-19 in the USA. Figures 1 and 5 show $\Xi$ as function of $\Upsilon$ of the diffusive trajectory time series of volatility and absolute log-return, respectively, for stock indexes. Figures 2 and 6 show $\Xi$ as function of $\Upsilon$ of the diffusive trajectory time series of volatility and absolute log-return, respectively, for currencies. Figures 3 and 7 show $\Xi$ as function of $\Upsilon$ of the diffusive trajectory time series of volatility and absolute log-return, respectively, for commodities and the treasure yield of the United States. Finally, Figs. 4 and 8 show $\Xi$ as function of $\Upsilon$ of the diffusive trajectory time series of volatility and absolute log-return, respectively, for the temperature and precipitation in Bogota, Colombia, and the daily cases and deaths of COVID-19 in the United States. Figures 1 and 5 show that $\Xi$ as function of $\Upsilon$ is strictly decreasing for the stock indexes NASDAQ, BOVESPA, and AEX, while in the rest of the cases it is observed that there is no general monotonic behavior. Figures 2 and 6 show that $\Xi$ as function of $\Upsilon$ is strictly nonincreasing for the Colombian peso-dollar (COP-USD) currency, while the euro-dollar (EUR-USD), pound sterling-dollar (GBP-USD), and dollar-yen (USD-JPY) show a strictly decreasing behavior characterized in the end by a plateau where the value of the variance stabilizes despite the value of the mean, and finally, the currency bitcoin-dollar (BTC-USD) shows nonmonotonic behavior. Figures 3 and 7 show that $\Xi$ as function of $\Upsilon$ is strictly decreasing for the treasure yield of the United States, while in commodities a nonmonotonic behavior is shown for gold and crude oil and a turning point for silver, which changes the behavior in this last time series. Finally, in Figs. 4 and 8 it is observed that $\Xi$ as function of $\Upsilon$ is strictly

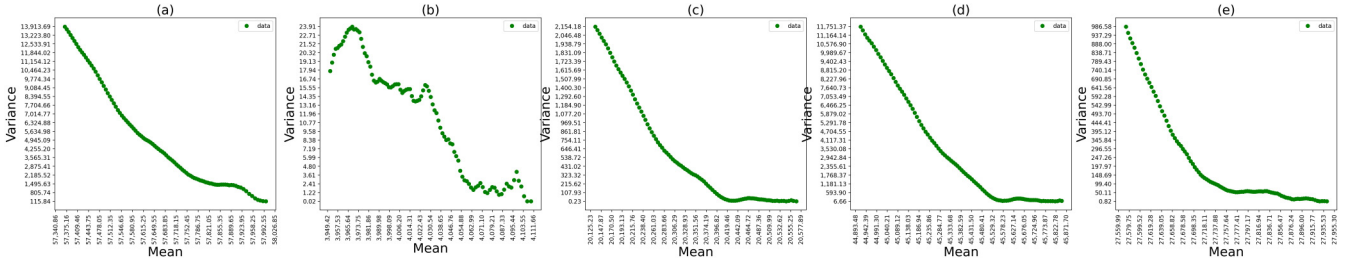


FIG. 2. Variance $\Xi$ as a function of the mean $\Upsilon$ for the diffusive trajectory time series of volatility of the: (a) Colombian peso-dollar (COP-USD), (b) bitcoin-dollar (BTC-USD), (c) euro-dollar (EUR-USD), (d) pound sterling-dollar (GBP-USD), and (e) dollar-yen (USD-JPY) currencies taking 100 time steps.

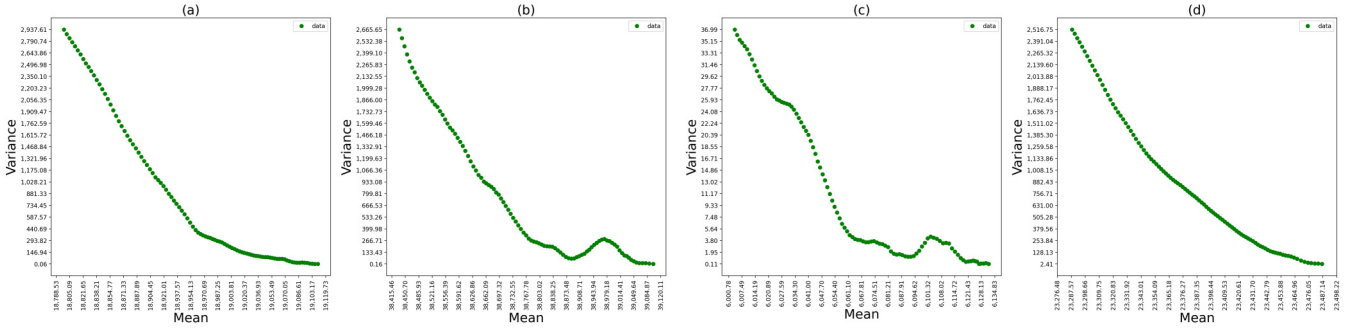


FIG. 3. Variance $\Xi$ as a function of the mean $\Upsilon$ for the diffusive trajectory time series of volatility of the: (a) silver, (b) gold, (c) crude oil commodities, and (d) the treasure yield of United States taking 100 time steps.

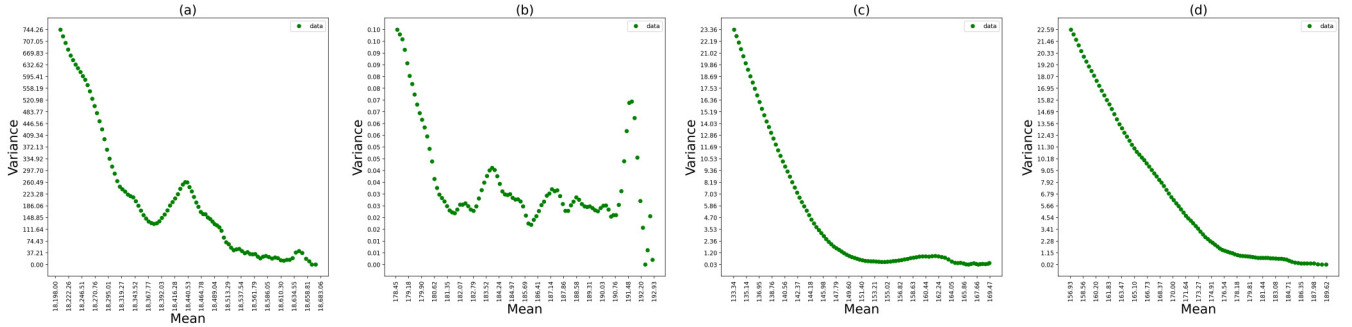


FIG. 4. Variance $\Xi$ as a function of the mean $\Upsilon$ for the diffusive trajectory time series of volatility of the: (a) temperature and precipitation in Bogota, Colombia, and (b) the daily cases and deaths of covid in the United States taking 100 time steps.

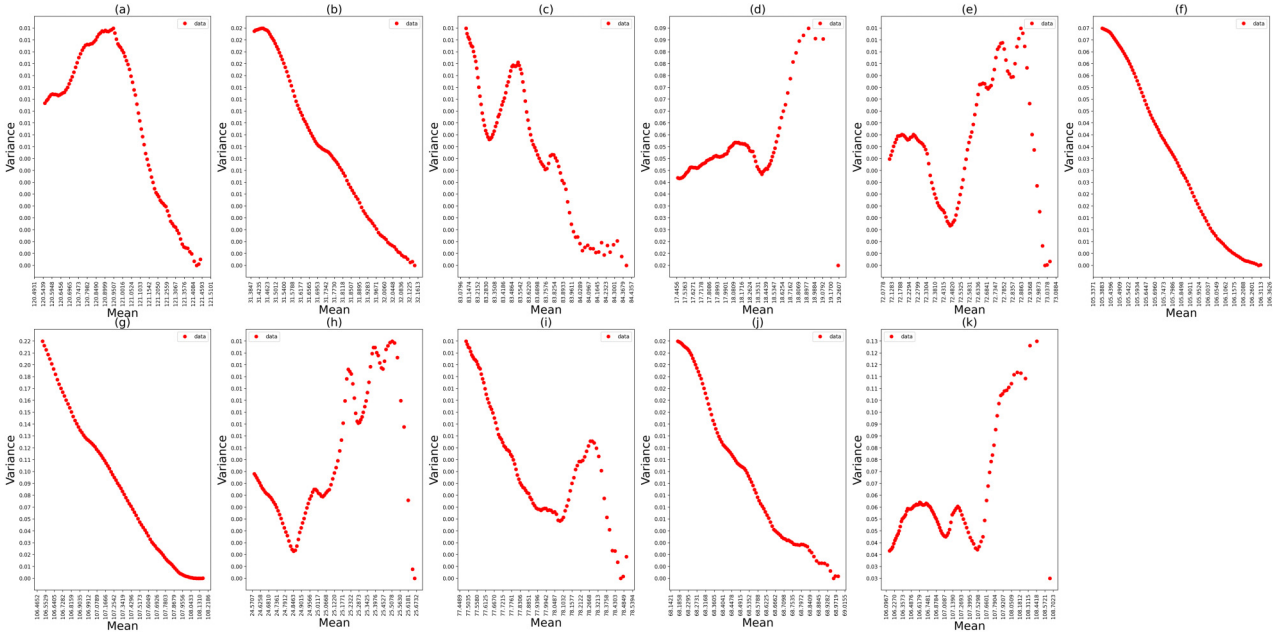


FIG. 5. Variance $\Xi$ as a function of the mean $\Upsilon$ for the diffusive trajectory time series of absolute log-return of the: (a) Nikkei 225, (b) S&P 500, (c) DAX, (d) MOEX, (e) IBEX 35, (f) NASDAQ, (g) BOVESPA, (h) COLCAP, (i) CAC 40, (j) AEX, and (k) RTS stock indexes taking 100 time steps.

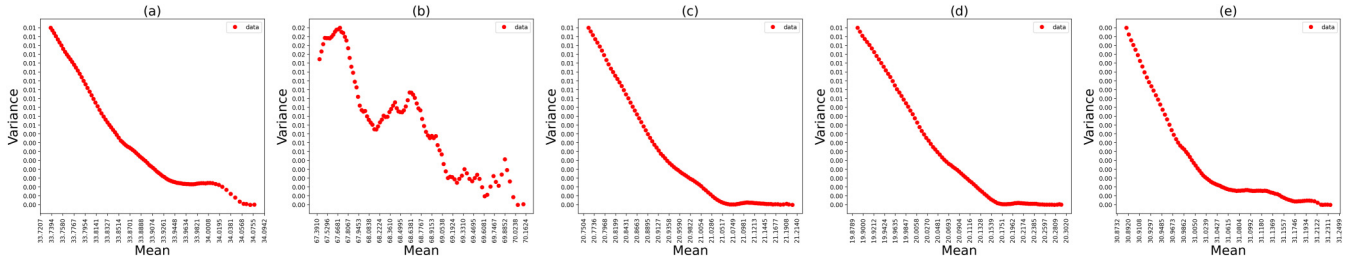


FIG. 6. Variance $\Xi$ as a function of the mean $\Upsilon$ for the diffusive trajectory time series of absolute log-return of the: (a) Colombian peso-dollar (COP-USD), (b) bitcoin-dollar (BTC-USD), (c) euro-dollar (EUR-USD), (d) pound sterling-dollar (GBP-USD), and (e) dollar-yen (USD-JPY) currencies taking 100 time steps.

decreasing for the daily deaths of COVID-19 in the United States, while for the temperature and precipitation in Bogota, Colombia, a nonmonotonic behavior is observed, and for the daily cases of COVID-19 in the United States, an inflection change is observed accompanied by a local minimum before the trend grows again. Therefore, it is clear that for the diffusive trajectory time series of volatility and absolute log-return of Nikkei 225, S&P 500, DAX, MOEX, IBEX 35, COLCAP, CAC 40, RTS, BTC-USD, EUR-USD, GBP-USD, USD-JPY, silver, gold, crude oil, the temperature in Bogota, precipitation in Bogota, and daily cases of COVID-19 in the United States, there are not strictly decreasing monotonic behaviors without inflection changes between $\Xi$ and $\Upsilon$. At this point, it is worth mentioning that it is quite clear that the TFS is a property that does not exist for diffusive trajectory time series, since it was not possible to adjust $\Xi$ as a function of $\Upsilon$ as a power-law relation of the form of Eq. (8) for any of the 24 time series considered in this work.

### B. Relation between Theil index and variance

Now, in this subsection we show that there is not an empirical relation between the normalized Theil index $T(t)/T(1)$ and $\Xi$. For this purpose, it is pertinent to mention that in all cases $T(1)$ turns out to be the maximum value of the Theil index throughout the different time steps taken. Thus, the same 24 time series are considered. Figures 9 and 13 show $T(t)/T(1)$ as a function of $\Xi$ of the diffusive trajectory time series of volatility and absolute log-return, respectively, for stock indexes. Figures 10 and 14 show $T(t)/T(1)$ as a function of $\Xi$ of the diffusive trajectory time series of volatility and absolute log-return, respectively, for currencies. Figures 11 and 15 show $T(t)/T(1)$ as a function of $\Xi$ of the diffusive trajectory time series of volatility and absolute log-return, respectively, for commodities and the treasure yield of the United States. Finally, Figs. 12 and 16 show $T(t)/T(1)$ as a function of $\Xi$ of the diffusive trajectory time series of volatility and absolute log-return, respectively, for the temperature and precipitation in Bogota, Colombia, and the daily cases and deaths of COVID-19 in the United States. Figures 9 and 13 show that the normalized Theil index as a function of the variance behaves strictly increasing for the S&P 500, NASDAQ, BOVESPA, and AEX stock indexes, while for the rest of the cases, it is observed that there is no a general monotonic behavior. Figures 10 and 14 show that the normalized Theil index as a function of the variance behaves strictly increasing for the Colombian peso-dollar (COP-USD), euro-dollar (EUR-USD), pound sterling-dollar (GBP-USD), and dollar-yen (USD-JPY), while the bitcoin-dollar currency (BTC-USD) shows nonmonotonic behavior. Figures 11 and 15 show that the normalized Theil index as a function of the variance behaves strictly increasing for the US Treasury yield and silver, while gold and crude oil exhibit nonmonotonic behavior. Finally, Figs. 12 and 16 show that the normalized Theil index as a function of the variance behaves strictly increasing for daily COVID-19 deaths in the United States, while for the temperature and precipitation in Bogotá, Colombia, a nonmonotonous behavior are observed, and for the daily cases of COVID-19 in the United States, an inflection change is observed accompanied by a trend that reduces the variance before it grows again. Therefore, it is clear that for the diffusive trajectory time series of volatility and absolute log-return of Nikkei 225, DAX, MOEX, IBEX 35, COLCAP, CAC 40, RTS, USD-JPY, gold, crude oil, temperature in

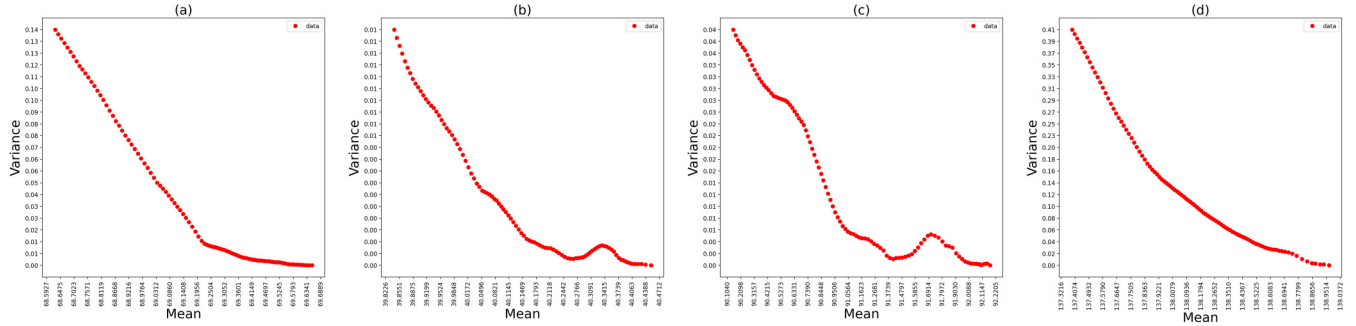


FIG. 7. Variance $\Xi$ as a function of the mean $\Upsilon$ for the diffusive trajectory time series of absolute log-return of the: (a) silver, (b) gold, (c) crude oil commodities, and (d) the treasure yield of United States taking 100 time steps.

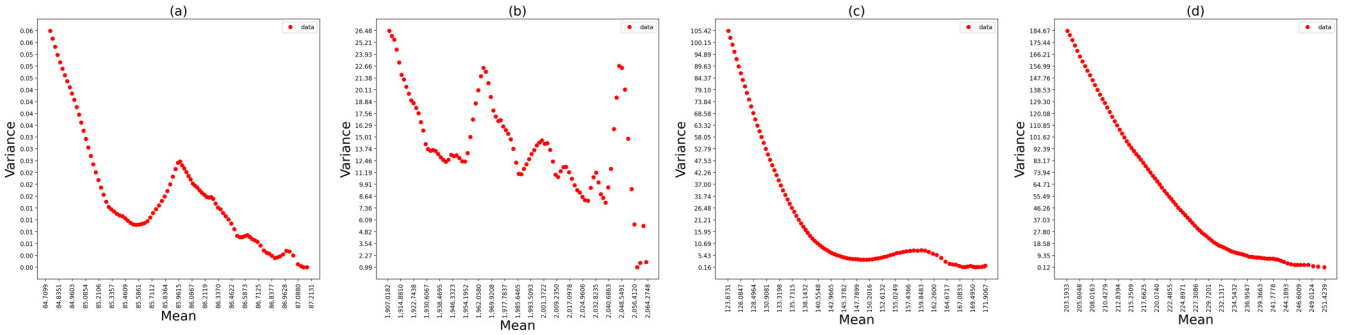


FIG. 8. Variance $\Xi$ as a function of the mean $\Upsilon$ for the diffusive trajectory time series of absolute log-return of the: (a) temperature and precipitation in Bogota, Colombia, and (b) the daily cases and deaths of covid in the United States taking 100 time steps.

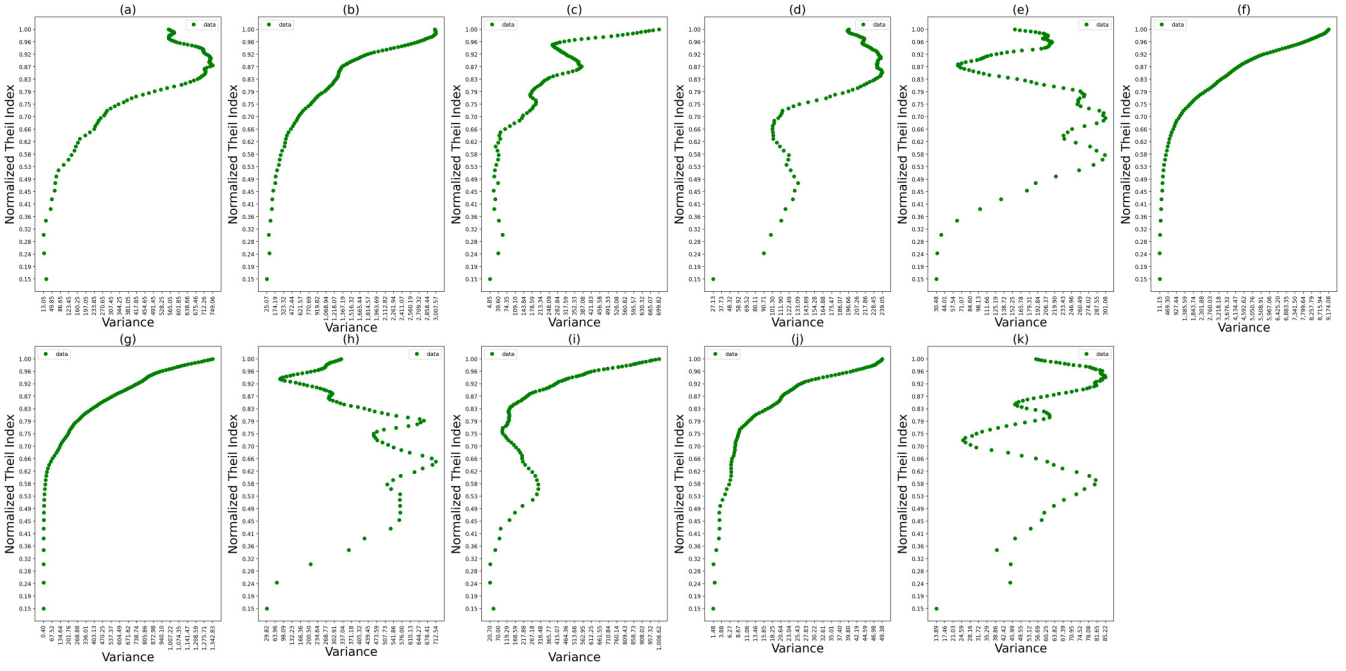


FIG. 9. Normalized Theil index $T(t)/T(1)$ as a function of the variance $\Xi$ for the diffusive trajectory time series of volatility of the: (a) Nikkei 225, (b) S&P 500, (c) DAX, (d) MOEX, (e) IBEX 35, (f) NASDAQ, (g) BOVESPA, (h) COLCAP, (i) CAC 40, (j) AEX, and (k) RTS stock indexes taking 100 time steps.

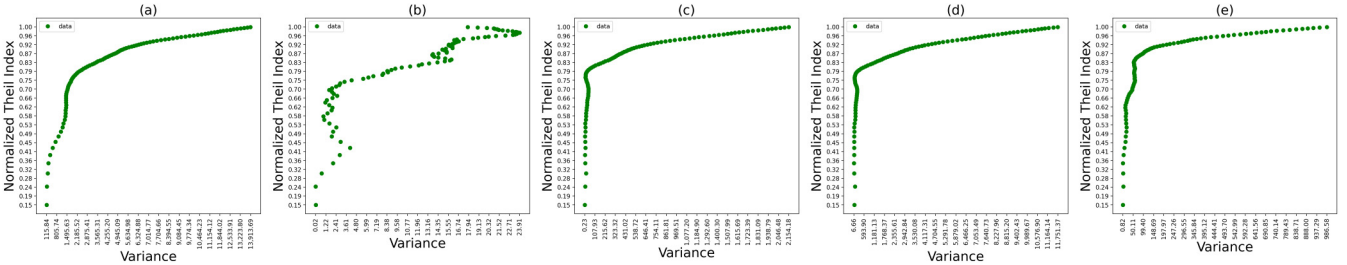


FIG. 10. Normalized Theil index $T(t)/T(1)$ as a function of the variance $\Xi$ for the diffusive trajectory time series of volatility of the: (a) Colombian peso-dollar (COP-USD), (b) bitcoin-dollar (BTC-USD), (c) euro-dollar (EUR-USD), (d) pound sterling-dollar (GBP-USD), and (e) dollar-yen (USD-JPY) currencies taking 100 time steps.

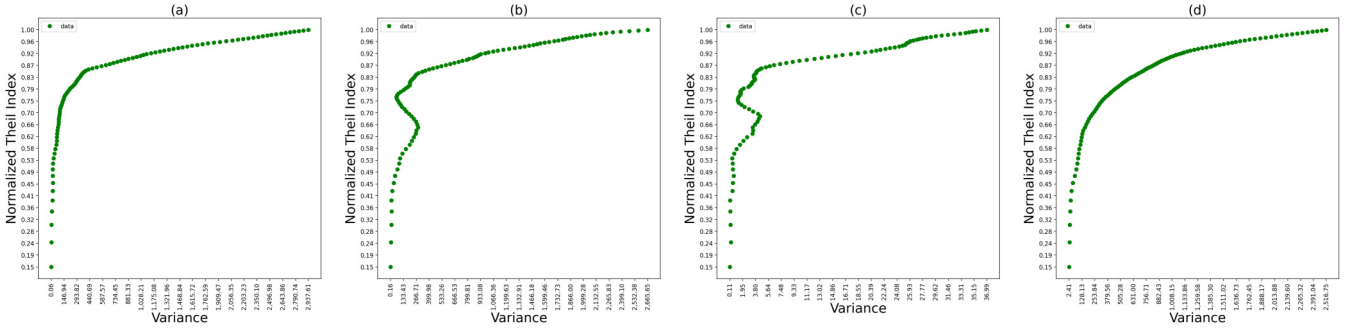


FIG. 11. Normalized Theil index $T(t)/T(1)$ as a function of the variance $\Xi$ for the diffusive trajectory time series of volatility of the: (a) silver, (b) gold, (c) crude oil commodities, and (d) the treasure yield of United States taking 100 time steps.

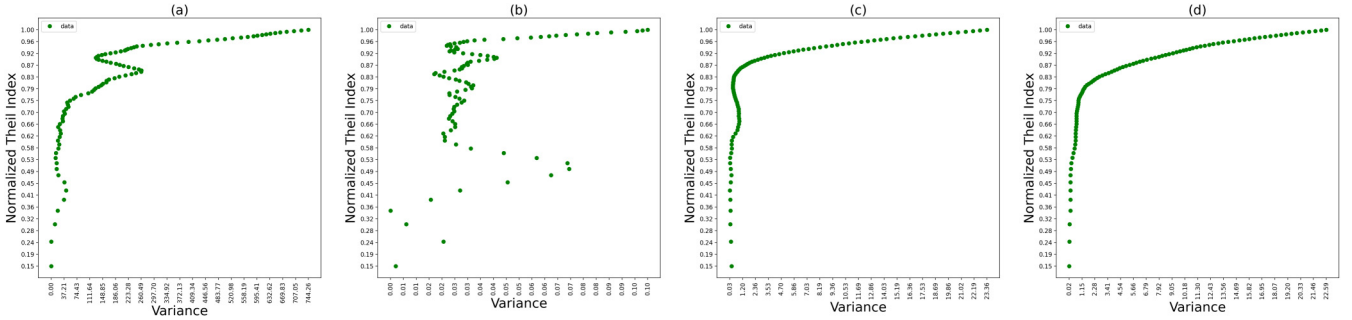


FIG. 12. Normalized Theil index $T(t)/T(1)$ as a function of the variance $\Xi$ for the diffusive trajectory time series of volatility of the: (a) temperature and precipitation in Bogota, Colombia, and (b) the daily cases and deaths of covid in the United States taking 100 time steps.

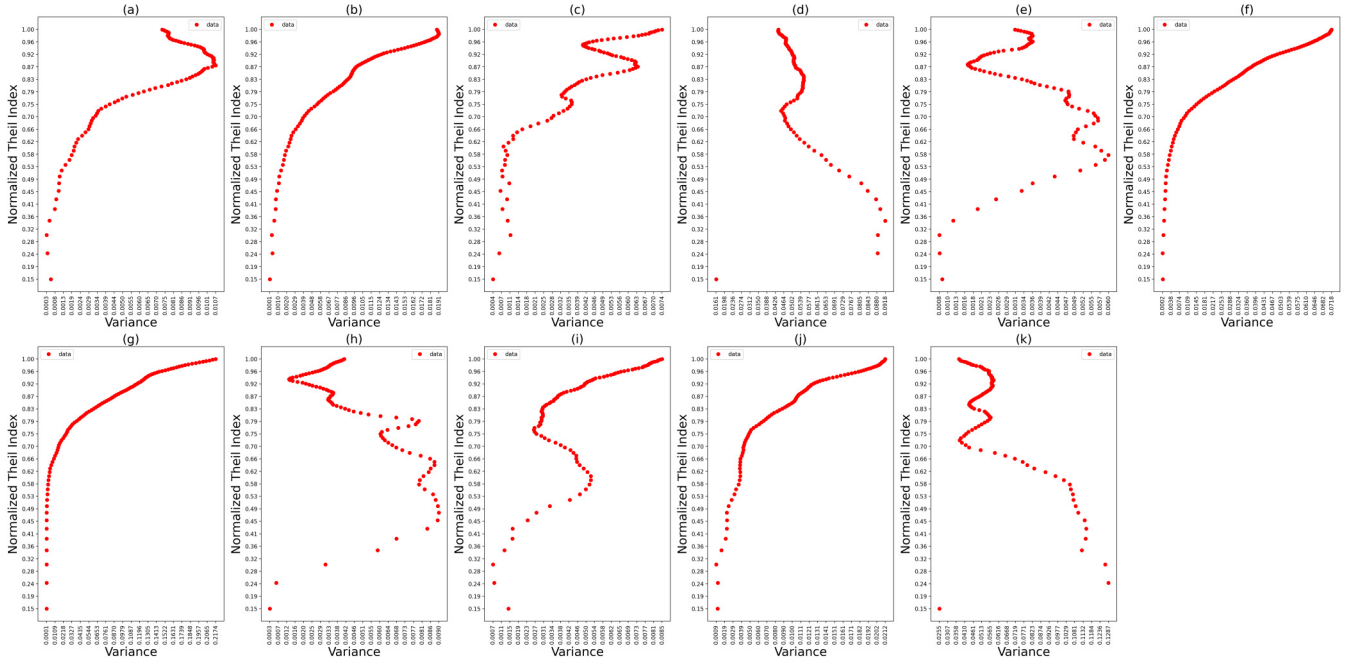


FIG. 13. Normalized Theil index $T(t)/T(1)$ as a function of the variance $\Xi$ for the diffusive trajectory time series of absolute log-return of the: (a) Nikkei 225, (b) S&P 500, (c) DAX, (d) MOEX, (e) IBEX 35, (f) NASDAQ, (g) BOVESPA, (h) COLCAP, (i) CAC 40, (j) AEX, and (k) RTS stock indexes taking 100 time steps.

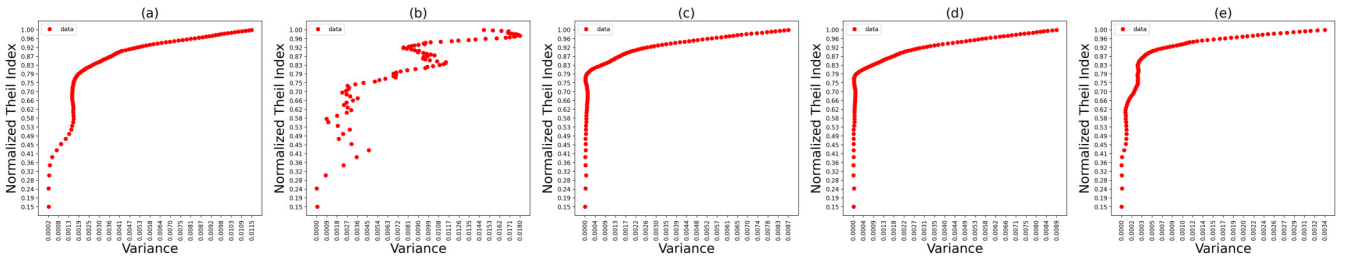


FIG. 14. Normalized Theil index $T(t)/T(1)$ as a function of the variance $\Xi$ for the diffusive trajectory time series of absolute log-return of the: (a) Colombian peso-dollar (COP-USD), (b) bitcoin-dollar (BTC-USD), (c) euro-dollar (EUR-USD), (d) pound sterling-dollar (GBP-USD), and (e) dollar-yen (USD-JPY) currencies taking 100 time steps.

Bogota, precipitation in Bogota, and daily cases of COVID-19 in the United States, there are not monotonic trends between $T(t)/T(1)$ and $\Xi$. In fact, it is observed that, in general, the diffusive trajectory time series of volatility and absolute log-return have similar trends that differ in the range of values that each time series takes. We emphasize that the analysis of the data show that does not exist a functional relation between $T(t)/T(1)$ and $\Xi$ for the diffusive trajectory time series of the 24 time series studied in this work.

### C. Relation between Theil index and mean

Finally, starting from the analysis of empirical data, we report the existence of a new temporal scaling in complex systems that we refer to as TTS. TTS is an empirical relation found between normalized $T$ and the normalized $\Upsilon$ for the diffusive trajectory time series of volatility and absolute log-return for all the 24 time series studied in this work, as it is shown in the Figs. 17–24. Figures 17 and 21 show $T(t)/T(1)$ as a function of normalized $\Upsilon$ of the diffusive trajectory time series of volatility and absolute log-return, respectively, for stock indexes. The Figs. 18 and 22 show $T(t)/T(1)$ as a function of normalized $\Upsilon$ of the diffusive trajectory time series of volatility and absolute log-return, respectively, for currencies. Figures 19 and 23 show $T(t)/T(1)$ as a function of normalized $\Upsilon$ of the diffusive trajectory time series of volatility and absolute log-return, respectively, for commodities and the treasure yield of the United States. Finally, Figs. 20 and 24 show $T(t)/T(1)$ as a function of normalized $\Upsilon$ of the diffusive trajectory time series of volatility and absolute log-return, respectively, for the temperature and precipitation in Bogota, Colombia, and the daily cases and deaths of COVID-19 in the United States. Figures 17–24 show that the normalized Theil index as a function of the mean behaves strictly decreasing for all diffusive trajectory time series of volatility and absolute log-return. The adjustments of the time series to a power-law relation of the form of Eq. (10) through a solid continuous line, corroborating the TTS in the diffusive trajectory time series (points) as an invariant law of scale. We think that this type of scaling could provide an approach to the origin of a temporal scaling that can be more easily related to the Hurst exponent, because this scaling is originated in time series that vary its window size, as it happens in the diffusive trajectory time series.

Tables II and III show for volatility and absolute log-return, respectively, the coefficients of the least-squares adjustment to the power-law relation given by Eq. (10), the global average error $\mathrm{GAE}_T(\%)$ given by Eq. (11) and the value of $\chi^2$ test given by Eq. (12) for each of the time series considered. The results shown in Tables II and III indicate that the constants $K_1$ of the TTS have different values and vary considerably, while the values of the exponents $\beta$ of the TTS are found in a small range between 0.26 and 0.54. The above indicates that the constant $K_1$ and the exponent $\beta$ of the TTS allow to characterize each time series. Additionally, the results show that if two time series have similar values of the exponent $\beta$, the correspondent values of the constant $K_1$ are different. This last fact can be illustrated, for instance, if we observe that the $\beta$ of Treasure yield of the United States for volatility is 0.3064 and the $\beta$ for daily deaths of COVID-19 in the United States is 0.3081, while for the first $K_1$ is 4.4410 and for the second $K_1$ is 1.7672. Also, for volatility and absolute log-return of daily cases and daily deaths of COVID-19 in the United States, we observe that the $K_1$ are smaller than 1.8, and these values

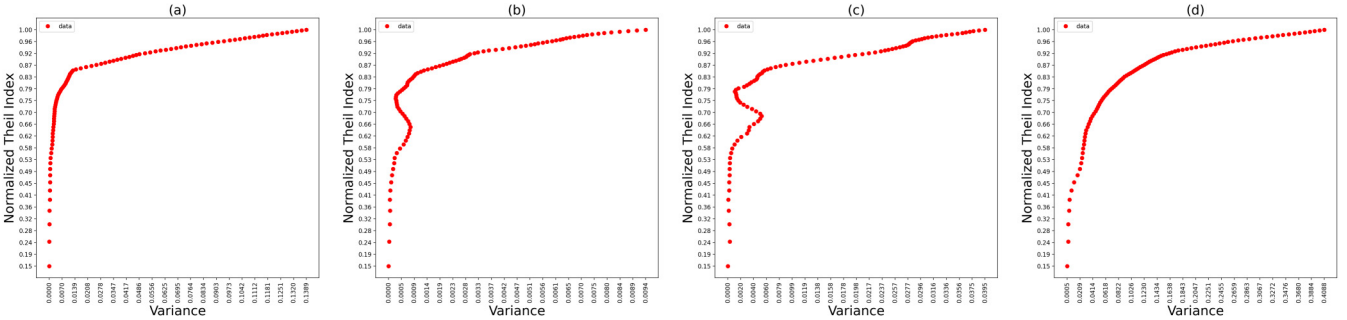


FIG. 15. Normalized Theil index $T(t)/T(1)$ as a function of the variance $\Xi$ for the diffusive trajectory time series of absolute log-return of the: (a) silver, (b) gold, (c) crude oil commodities, and (d) the treasure yield of United States taking 100 time steps.

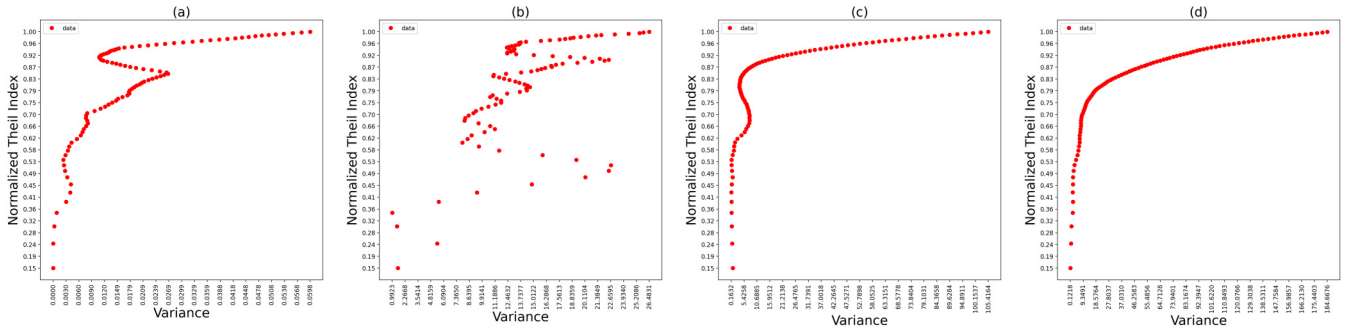


FIG. 16. Normalized Theil index $T(t)/T(1)$ as a function of the variance $\Xi$ for the diffusive trajectory time series of absolute log-return of the: (a) temperature and precipitation in Bogota, Colombia, and (b) the daily cases and deaths of covid in the United States taking 100 time steps.

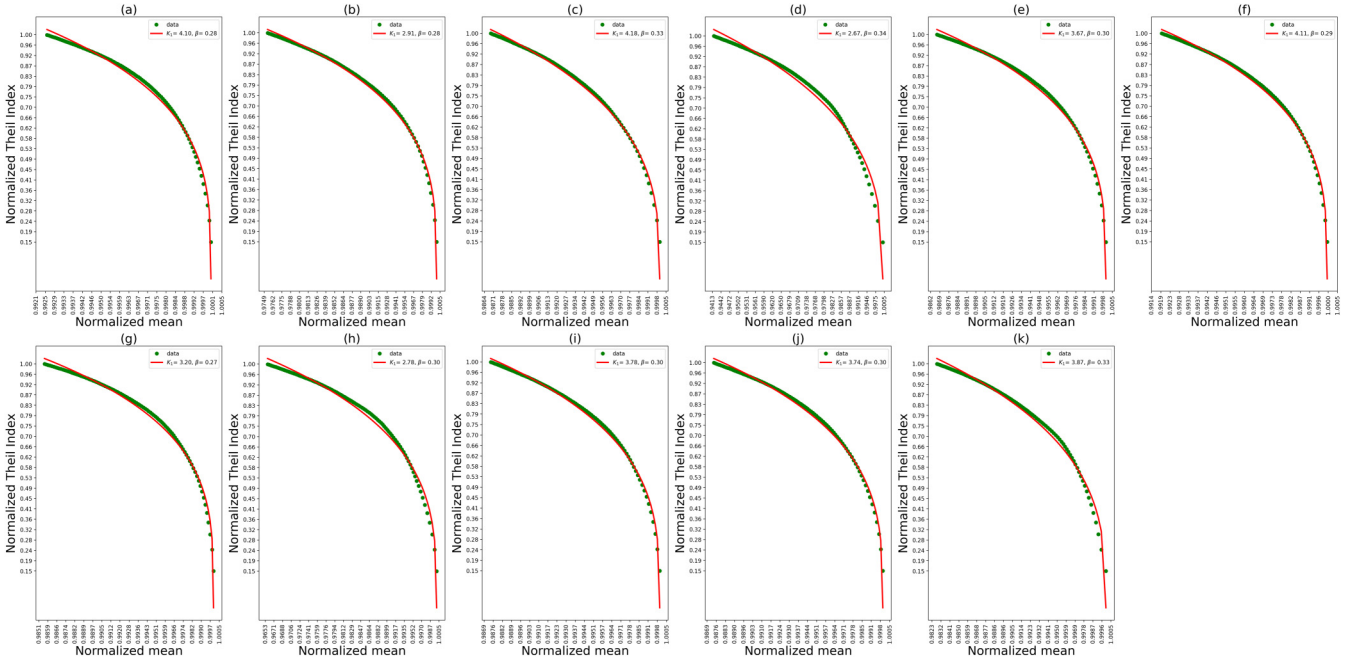


FIG. 17. Normalized Theil index $T(t)/T(1)$ as a function of the normalized mean $\Upsilon(t)/\Upsilon_M$ for the diffusive trajectory time series of volatility of the: (a) Nikkei 225, (b) S&P 500, (c) DAX, (d) MOEX, (e) IBEX 35, (f) NASDAQ, (g) BOVESPA, (h) COLCAP, (i) CAC 40, (j) AEX, and (k) RTS stock indexes taking 100 time steps. Red line: fit with Eq. (10). Green line: Empirical data.

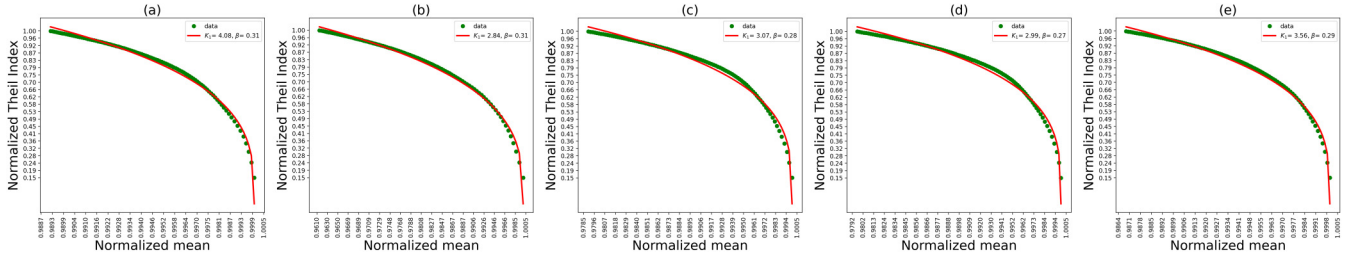


FIG. 18. Normalized Theil index $T(t)/T(1)$ as a function of the normalized mean $\Upsilon(t)/\Upsilon_M$ for the diffusive trajectory time series of volatility of the: (a) Colombian peso-dollar (COP-USD), (b) bitcoin-dollar (BTC-USD), (c) euro-dollar (EUR-USD), (d) pound sterling-dollar (GBP-USD), and (e) dollar-yen (USD-JPY) currencies taking 100 time steps. Red line: fit with Eq. (10). Green line: Empirical data.

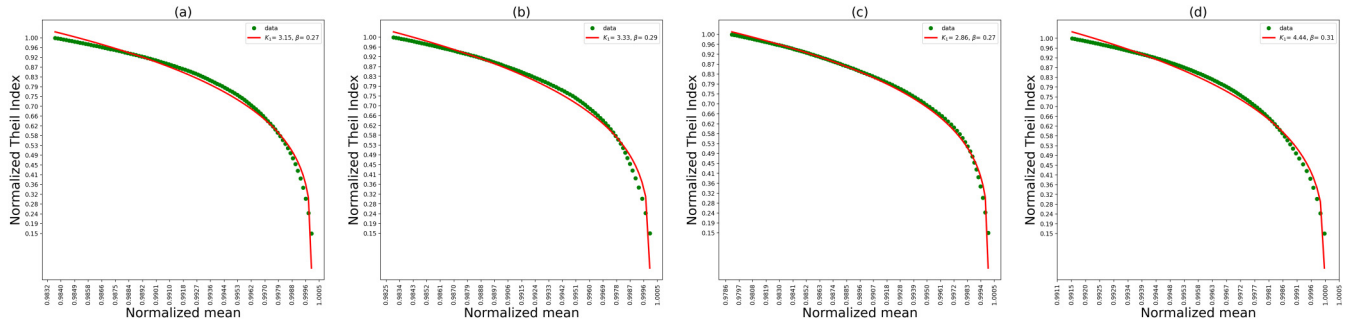


FIG. 19. Normalized Theil index $T(t)/T(1)$ as a function of the normalized mean $\Upsilon(t)/\Upsilon_M$ for the diffusive trajectory time series of volatility of the: (a) silver, (b) gold, (c) crude oil commodities, and (d) the treasure yield of United States taking 100 time steps. Red line: fit with Eq. (10). Green line: Empirical data.

are smallest for all the systems considered. Additionally, we observe that $K_1$ and $\beta$ are higher in daily deaths than in daily cases of COVID-19, which seems to indicate that $\beta$ may be related with the temporal correlation, given that daily deaths are easier to project than daily cases of COVID-19. Finally, we observed that GAE(%) is less than 4.6% in all the cases, which together with the value of $\chi^2$, it demonstrates the good quality of the TTS fit. Actually, the smallest value of GAE(%) is obtained for the time series of daily cases of COVID-19 in the United States for the case of volatility, while for the case of absolute log-return the smallest value of GAE(%) is obtained for DAX stock index.

## IV. GINZBURG-LANDAU THEORY AND TTS

In the context of condensed matter physics, it is a known fact that the Ginzburg-Landau theory allows to describe second-order phase transitions from the group of symmetries obeyed by the Hamiltonian of the system [35]. This description starts from the free-energy density in which the Hamiltonian of the system is expressed through a parameter of order $\psi$ and which, in the context of superconductivity theory, can be related to the Cooper pair density [36]. Then, by calculating the nontrivial critical points of the free-energy functional, different power-laws can be obtained for different thermodynamic variables around the value of the critical temperature $\theta_c$ in terms of phenomenological parameters and the so-called critical exponents of the system. In particular, $\|\psi\| \sim (1-\theta/\theta_c)^{\gamma}$ is obtained for $\theta < \theta_c$, where $\theta$ is the temperature of the system, which implies a universal exponent $\gamma = 1/2$ [36]. However, different physical systems show that this exponent does not have a single value but depends on the system, namely, in superconductivity $\gamma = 1/2$ [36], in ferroelectric systems $\gamma \in [0.33, 0.34]$ [37], in binary alloys $\gamma = 0.305 \pm 0.005$ [38], in binary fluid mixtures $\gamma \in [0.30, 0.34]$ [39], in gas-liquid systems $\gamma \in [0.32, 0.35]$ [39], and in magnetic systems $\gamma \in [0.30, 0.36]$ [40]. However, we have found, for the case of diffusive trajectory time series of volatility, that the values of TTS exponent $\beta$ are in the range $\beta \in [0.26, 0.34]$, while for the diffusive trajectory time series of absolute log-return, the values of $\beta$ are in the range $\beta \in [0.25, 0.54]$. Thus, the TTS exponents have, surprisingly, values in a range which is very close to the observed range for $\gamma$ for different physical systems [36,40]. Even so, it is not superfluous to mention that there are approximations of the Ginzburg-Landau theory for the corrections of the critical exponents according to the dimensionality $d$, as it is shown in Table 3 of Ref. [41]. Also, to describe phase transitions of order $p > 2$, it is useful to take even powers of the norm of the order parameter $\psi$ greater than 4 at the free energy $F$, that is, $F \sim \|\psi\|^{2p}$, with $p > 2$ as suggested in Ref. [42]. Therefore, with the above motivation, added to the fact that the theory of Ginzburg-Landau allows to explain the difference between systems in terms of phenomenological parameters, the following free-energy functional $\mathcal{F}_{\eta,\delta}$ is introduced:

$$\mathcal{F}_{\eta,\delta} = \frac{a_{\eta,\delta}}{2}\|\psi\|^{\eta} + b_{\eta,\delta}\|\psi\|^{\delta} - c_{\eta,\delta}\|\psi\|, \tag{13}$$

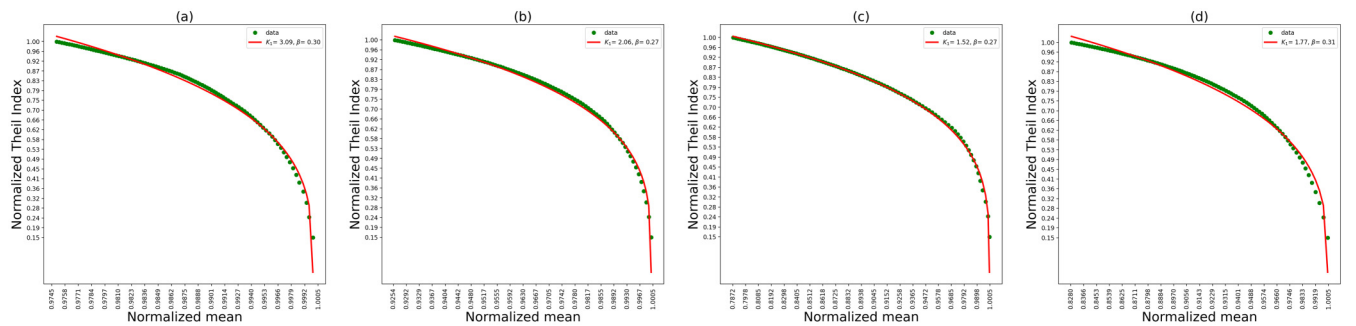


FIG. 20. Normalized Theil index $T(t)/T(1)$ as a function of the normalized mean $\Upsilon(t)/\Upsilon_M$ for the diffusive trajectory time series of volatility of the: (a) temperature and precipitation in Bogota, Colombia, and (b) the daily cases and deaths of covid in the United States taking 100 time steps. Red line: fit with Eq. (10). Green line: Empirical data.

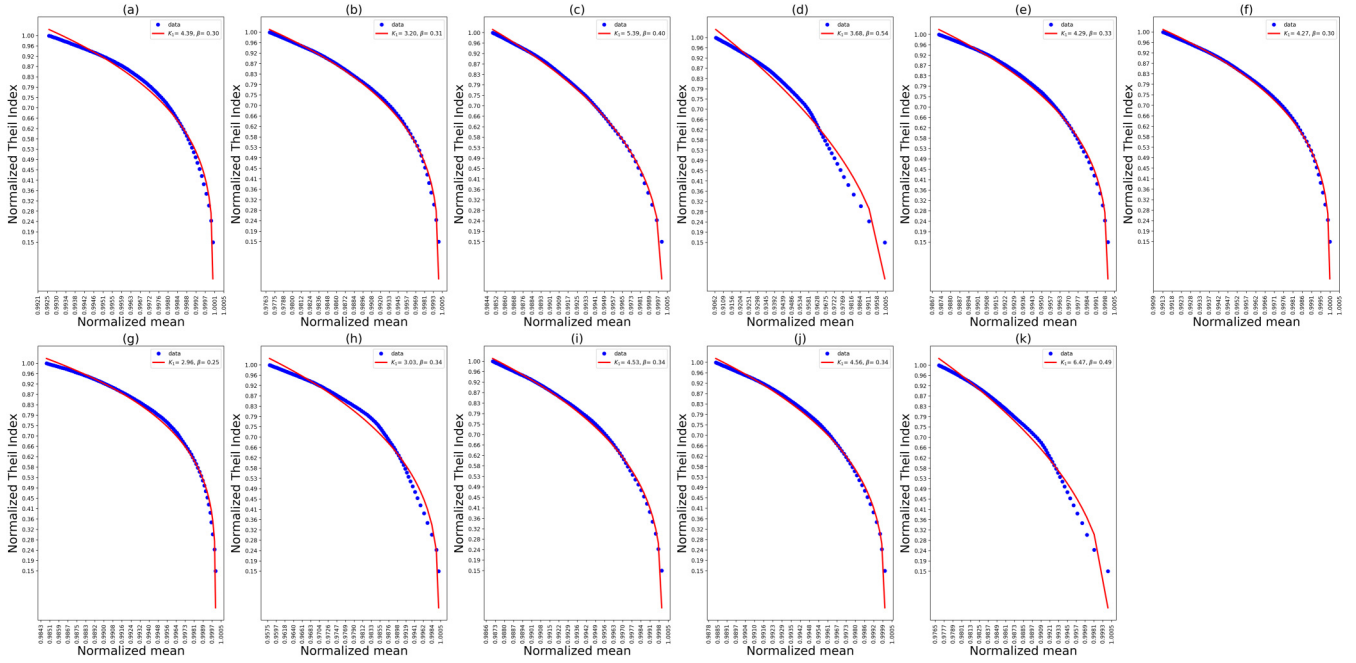


FIG. 21. Normalized Theil index $T(t)/T(1)$ as a function of the normalized mean $\Upsilon(t)/\Upsilon_M$ for the diffusive trajectory time series of absolute log-return of the: (a) Nikkei 225, (b) S&P 500, (c) DAX, (d) MOEX, (e) IBEX 35, (f) NASDAQ, (g) BOVESPA, (h) COLCAP, (i) CAC 40, (j) AEX, and (k) RTS stock indexes taking 100 time steps. Red line: fit with Eq. (10). Blue line: Empirical data.

where $\delta > \eta > 0$, $a_{\eta,\delta}$, $b_{\eta,\delta}$, and $c_{\eta,\delta}$ are parameters. Also, $\eta$ and $\delta$, which are related with the critical exponent $\beta$, $a_{\eta,\delta}$, $b_{\eta,\delta}$, and $c_{\eta,\delta}$, are phenomenological parameters that depend on $\tau = \frac{\theta_c - \theta}{\theta_c}$, a transition parameter defined through the temperature $\theta$ and the critical temperature $\theta_c$, and $\psi$ is the order parameter such that if $\theta > \theta_c$, then $\psi$ becomes zero. From Eq. (13) and for the case $c_{\eta,\delta} = 0$, it is easy to verify the existence of a nontrivial critical point

$$\|\psi\|^{\delta-\eta} = -\frac{\eta a_{\eta,\delta}}{2\delta b_{\eta,\delta}}. \tag{14}$$

In particular, if we assume that $a_{\eta,\delta}$ and $b_{\eta,\delta}$ vary smoothly enough with respect to $\tau$, that is, $a_{\eta,\delta} = -a^{(0)}_{\eta,\delta}\tau$ and $b_{\eta,\delta} = b^{(0)}_{\eta,\delta}$, then the expression Eq. (14) can be reduced to

$$\|\psi\| = \left(\frac{\eta a^{(0)}_{\eta,\delta}}{2\delta b^{(0)}_{\eta,\delta}}\right)^{\frac{1}{\delta-\eta}} \left\|1 - \frac{\theta}{\theta_c}\right\|^{\frac{1}{\delta-\eta}}, \tag{15}$$

which is identical to $\|\psi\| \sim (1-\theta/\theta_c)^{\gamma}$ when $\gamma^{-1} = \delta - \eta$. Thus, this new way of writing the power-law for the exponent $\gamma$ and the order parameter $\|\psi\|$ in terms of some new exponents $\eta$ and $\delta$, allow to explain a larger range of values for $\gamma$. For example, if $\eta = 2$ and $\delta = 4$, then the classical result of $\gamma = 1/2$ is returned. In addition, if $(\eta, \delta) = (4, 6)$ or $(\eta, \delta) = (6, 8)$ as in Ref. [42], so $\gamma = 1/2$. However, one could also have possibilities like $\eta = 3$ and $\delta = 6$ such that $\gamma = 0.33$, which is closer to the value of $\gamma$ for some physical systems [36–40]. We note that terms of the form $\|\psi\|^3$ do not violate invariance under spatial rotations. However, the theoretical result given by Eq. (15) for condensed matter systems has the same functional form as the empirical result given by Eq. (10), when $\|\psi\| = \frac{T(t)}{T(1)}$, $K_1^{\delta-\eta} = \frac{\eta a^{(0)}_{\eta,\delta}}{2\delta b^{(0)}_{\eta,\delta}}$, and $\gamma = \beta$ for complex systems. Therefore, it is possible to explain the difference between the exponent $\beta$ and the constant $K_1$ of the TTS, by observing that the latter is the variable

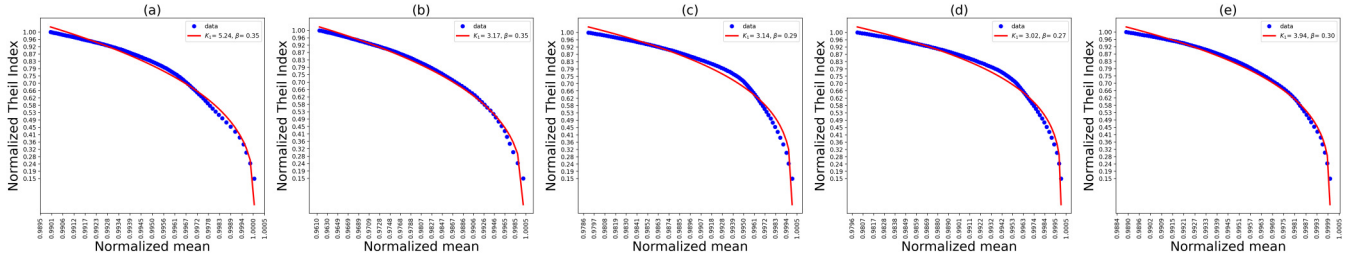


FIG. 22. Normalized Theil index $T(t)/T(1)$ as a function of the normalized mean $\Upsilon(t)/\Upsilon_M$ for the diffusive trajectory time series of absolute log-return of the: (a) Colombian peso-dollar (COP-USD), (b) bitcoin-dollar (BTC-USD), (c) euro-dollar (EUR-USD), (d) pound sterling-dollar (GBP-USD), and (e) dollar-yen (USD-JPY) currencies taking 100 time steps. Red line: fit with Eq. (10). Blue line: Empirical data.

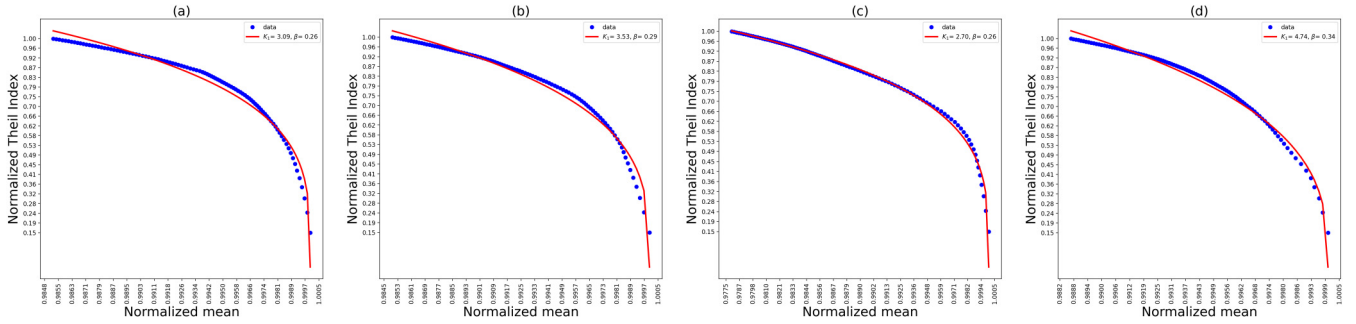


FIG. 23. Normalized Theil index $T(t)/T(1)$ as a function of the normalized mean $\Upsilon(t)/\Upsilon_M$ for the diffusive trajectory time series of absolute log-return of the: (a) silver, (b) gold, (c) crude oil commodities, and (d) the treasure yield of United States taking 100 time steps. Red line: fit with Eq. (10). Blue line: Empirical data.

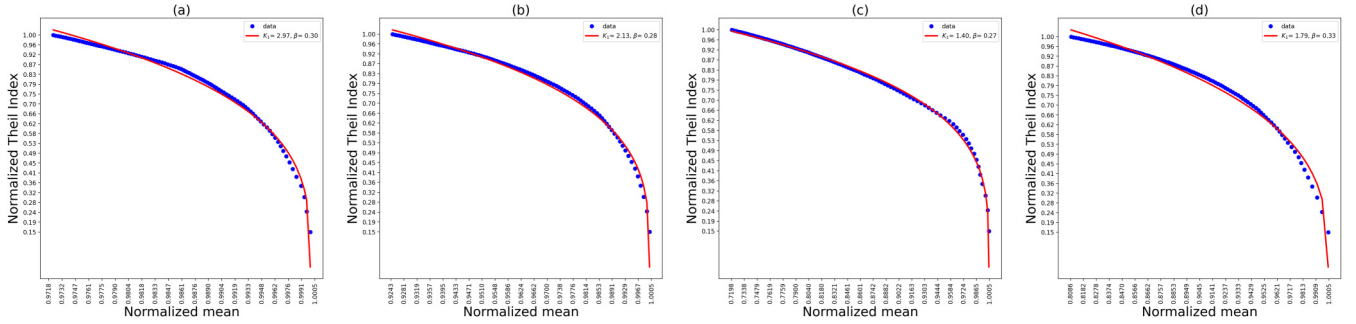


FIG. 24. Normalized Theil index $T(t)/T(1)$ as a function of the normalized mean $\Upsilon(t)/\Upsilon_M$ for the diffusive trajectory time series of absolute log-return of the: (a) temperature and precipitation in Bogota, Colombia, and (b) the daily cases and deaths of covid in the United States taking 100 time steps. Red line: fit with Eq. (10). Blue line: Empirical data.

TABLE II. $K_1$ and $\beta$ adjustment parameters of the TTS [see Eq. (10)] for the diffusive trajectory time series of volatility of the Nikkei 225, S&P 500, DAX, MOEX, IBEX 35, NASDAQ, BOVESPA, COLCAP, CAC 40, AEX, and RTS stock indexes, the Colombian peso-dollar (COP-USD), bitcoin-dollar (BTC-USD), euro-dollar (EUR-USD), pound sterling-dollar (GBP-USD), dollar-yen (USD-JPY) currencies, the silver, gold, crude oil commodities, the treasure yield of United States, the temperature and precipitation in Bogota, Colombia, and the daily cases and deaths of COVID-19 in the United States taking 100 time steps.

| Time Series | $K_1$ | $\beta$ | GAE(%) | $\chi^2$ |
|---|---|---|---|---|
| Nikkei 225 | 4,0981±0.0996 | 0.2835±0.0044 | 3,0287 | 0.1967 |
| S&P 500 | 2,9111±0.0482 | 0.2847±0.0038 | 2,4218 | 0.1781 |
| DAX | 4,1777±0.0875 | 0.3263±0.0043 | 2,3262 | 0.1717 |
| MOEX | 2,6706±0.0568 | 0.3362±0.0062 | 3,8149 | 0.2475 |
| IBEX 35 | 3,6693±0.0790 | 0.2961±0.0043 | 2,8372 | 0.1907 |
| NASDAQ | 4,1137±0.0891 | 0.2901±0.0040 | 2,5263 | 0.1807 |
| BOVESPA | 3,2030±0.0653 | 0.2694±0.0041 | 2,9554 | 0.1996 |
| COLCAP | 2,7757±0.0549 | 0.2955±0.0049 | 3,3215 | 0.2114 |
| CAC 40 | 3,7844±0.0775 | 0.3012±0.0041 | 2,5474 | 0.1799 |
| AEX | 3,7360±0.0757 | 0.2973±0.0041 | 2,5306 | 0.1761 |
| RTS | 3,8714±0.0980 | 0.3281±0.0055 | 3,3145 | 0.2288 |
| USD-COP | 4,0795±0.0992 | 0.3055±0.0047 | 3,0563 | 0.1945 |
| BTC-USD | 2,8411±0.0501 | 0.3146±0.0046 | 2,7518 | 0.1941 |
| EUR-USD | 3,0711±0.0724 | 0.2838±0.0052 | 3,7530 | 0.2410 |
| GBP-USD | 2,9894±0.0674 | 0.2743±0.0049 | 3,6527 | 0.2281 |
| USD-JPY | 3,5605±0.0798 | 0.2875±0.0045 | 3,0817 | 0.2031 |
| Silver | 3,1480±0.0714 | 0.2724±0.0047 | 3,4864 | 0.2279 |
| Gold | 3,3255±0.0797 | 0.2893±0.0051 | 3,5291 | 0.2392 |
| Crude Oil | 2,8565±0.0483 | 0.2683±0.0037 | 2,4248 | 0.1933 |
| Treasure Yield U.S. | 4,4410±0.1226 | 0.3064±0.0051 | 3,3643 | 0.2109 |
| Bogota Temperature | 3,0882±0.0604 | 0.2995±0.0045 | 2,9192 | 0.1938 |
| Bogota precipitation | 2,0561±0.0259 | 0.2709±0.0038 | 2,6672 | 0.1866 |
| Covid Cases USA | 1,5159±0.0108 | 0.2653±0.0032 | 1,7125 | 0.1614 |
| Covid Deaths USA | 1,7672±0.0217 | 0.3081±0.0051 | 3,2799 | 0.2132 |

TABLE III. $K_1$ and $\beta$ adjustment parameters of the TTS [see Eq. (10)] for the diffusive trajectory time series of absolute log-return of the Nikkei 225, S&P 500, DAX, MOEX, IBEX 35, NASDAQ, BOVESPA, COLCAP, CAC 40, AEX, and RTS stock indexes, the Colombian peso-dollar (COP-USD), bitcoin-dollar (BTC-USD), euro-dollar (EUR-USD), pound sterling-dollar (GBP-USD), dollar-yen (USD-JPY) currencies, the silver, gold, crude oil commodities, the treasure yield of United States, the temperature and precipitation in Bogota, Colombia, and the daily cases and deaths of COVID-19 in the United States taking 100 time steps.

| Time Series | $K_1$ | $\beta$ | GAE(%) | $\chi^2$ |
|---|---|---|---|---|
| Nikkei 225 | 4,3937±0.1193 | 0.2964±0.0049 | 3,2884 | 0.2048 |
| S&P 500 | 3,2044±0.0553 | 0.3064±0.0040 | 2,2623 | 0.1739 |
| DAX | 5,3874±0.1201 | 0.3984±0.0048 | 1,8793 | 0.1591 |
| MOEX | 3,6795±0.1137 | 0.5353±0.0112 | 4,4052 | 0.2732 |
| IBEX 35 | 4,2887±0.0959 | 0.3296±0.0045 | 2,5600 | 0.1750 |
| NASDAQ | 4,2715±0.0888 | 0.3035±0.0039 | 2,2074 | 0.1716 |
| BOVESPA | 2,9590±0.0538 | 0.2545±0.0037 | 2,6853 | 0.1902 |
| COLCAP | 3,0303±0.0733 | 0.3413±0.0065 | 3,6925 | 0.2341 |
| CAC 40 | 4,5257±0.0951 | 0.3444±0.0043 | 2,1569 | 0.1643 |
| AEX | 4,5630±0.1012 | 0.3374±0.0044 | 2,3420 | 0.1678 |
| RTS | 6,4680±0.2407 | 0.4876±0.0089 | 3,7416 | 0.2464 |
| USD-COP | 5,2412±0.1630 | 0.3531±0.0060 | 3,3283 | 0.2004 |
| BTC-USD | 3,1673±0.0610 | 0.3480±0.0051 | 2,7436 | 0.1950 |
| EUR-USD | 3,1365±0.0903 | 0.2872±0.0063 | 4,5848 | 0.3000 |
| GBP-USD | 3,0152±0.0774 | 0.2736±0.0055 | 4,1862 | 0.2573 |
| USD-JPY | 3,9384±0.0927 | 0.2980±0.0046 | 2,9871 | 0.1936 |
| Silver | 3,0878±0.0858 | 0.2594±0.0056 | 4,4626 | 0.2953 |
| Gold | 3,5263±0.1023 | 0.2937±0.0060 | 4,1470 | 0.2941 |
| Crude Oil | 2,6979±0.0464 | 0.2594±0.0038 | 2,4971 | 0.2081 |
| Treasure Yield U.S. | 4,7363±0.1385 | 0.3398±0.0058 | 3,3689 | 0.2041 |
| Bogota Temperature | 2,9674±0.0587 | 0.2972±0.0047 | 3,1071 | 0.1995 |
| Bogota precipitation | 2,1271±0.0291 | 0.2847±0.0042 | 2,8777 | 0.1914 |
| Covid Cases USA | 1,3988±0.0090 | 0.2676±0.0033 | 1,9184 | 0.1606 |
| Covid Deaths USA | 1,7903±0.0235 | 0.3339±0.0058 | 3,4858 | 0.2257 |

that depends on phenomenological parameters as $a^{(0)}_{\eta,\delta}$ and $b^{(0)}_{\eta,\delta}$. Indeed, the values for $\beta$ reported in Tables II and III suggest that the value of the difference of the critical exponents $\delta - \eta$ is similar in most time series, and that the most noticeable difference of the constant of the TTS, $K_1$, comes from the phenomenological parameters $a^{(0)}_{\eta,\delta}$ and $b^{(0)}_{\eta,\delta}$, which must be different for each diffusive trajectory time series. Finally, it is clear that $\tau = 1 - \theta/\theta_c$ plays the role analogous to the quantity $1 - \Upsilon(t)/\Upsilon_M$ in the TTS [see Eq. (10)], which is in agreement with the fact that temperature represents a statistical average in complex systems, and $\theta_c$ is the maximum temperature when $\theta < \theta_c$.

## V. CONCLUSIONS

We have shown in Sec. III A the TFS analysis for the 24 diffusive trajectory time series considered in this work, which implies a window size on the data that varies over time in such a way that two facts are obtained to highlight: (i) a possible relation with the Hurst exponent is more evident as it is a time series with a moving window, and (ii) TFS is a property that has been proposed in cumulative time series, where the power-law relation relation between $\Xi$ and $\Upsilon$ is satisfied [1,9], while in the diffusive trajectory time series this type of power-law does not exist. In fact, it is observed that in 18 of the 24 time series used, there is no strictly decreasing monotonic behavior without inflection changes, but that there are some peaks or plateaus (see Figs. 1–8). In Sec. III B, we have exposed the relation between $T(t)/T(1)$ and $\Xi$, which was in agreement with the fact reported in literature [24,25] in the sense that $T$ is related with $\Xi$ for different probability density functions. However, it is also clear that in all the cases there is not functional behavior between $T$ and $\Xi$. In fact, it is observed that in 17 of the 24 time series used, there is no strictly increasing behavior but there are some peaks (see Figs. 9–16). Also, the time series of diffusive trajectory for volatility and absolute log-return have similar trends that differ in the range of values that each time series takes. In Sec. III C, we have shown the new form of temporal scaling found for nonstationary time series, that we have called as TTS. Even so, this behavior should be an universal behavior in complex systems that establishes a point of view closer to the concepts of econophysics. Therefore, the irregular behavior of $T(t)/T(1)$ as a function of $\Xi$ is compensated by the regular behavior of $T(t)/T(1)$ as a function of $\Upsilon$. In this sense, it is observed that the exponent $\beta$ and the constant $K_1$ of the TTS allow to characterize different time series. Thus, for the nonstationary time series of diffusive trajectory studied in this work, we have found $\beta \in [0.26, 0.34]$ and $K_1 \in [1.51, 4.45]$ for volatility, and $\beta \in [0.25, 0.54]$ and $K_1 \in [1.40, 6.47]$ for absolute log-return. At this point, we have shown that the GAE(%) is less than 4.6% in all the cases and so we have corroborated the goodness of fit for TTS. Furthermore, it is worth mentioning that Eq. (15) characterizes the TTS as an emergent macroscopic property of a microscopic dynamics, where the temperature $\theta$ is analogous to the mean $\Upsilon(t)$, the

critical temperature $\theta_c$ is analogous to the maximum mean $\Upsilon_M$, and the order parameter $\|\psi\|$ is analogous to the normalized Theil index $T(t)/T(1)$ for $\theta < \theta_c$. Also, the Eq. (15) allows to establish the constant $K_1$ as a variable that depends on phenomenological parameters of the different time series, as it is evidenced in Tables II and III, while the exponent $\beta$ is associated with the difference of the critical exponents $\delta - \eta$, which is associated with the range of values observed. Thus, we can assume that the exponent $\beta$ obtained from the empirical relation of the TTS could be interpreted as a critical exponent $\gamma$ in complex systems, such that $\beta$ covers broader values than those reported in the condensed matter literature [36–40], suggesting that physical phenomena such as $\gamma \in [0.25, 0.30)$ and $\gamma \in (0.5, 0.54]$ might exist. More generally, since the derivation of Eq. (15) from the nontrivial critical points of the energy functional $\mathcal{F}_{\eta,\delta}$ of Eq. (13), which is valid from condensed matter physics, this expression is a result that allows us to understand an arbitrary exponent $\gamma$ and suggests the use of fractional calculus in the Ginzburg-Landau theory, since $\eta$ and $\delta$ can take noninteger values. Finally, we expect to be able to study TTS using a complete analytical model that be independent of the type of complex system considered. This last idea would be consistent with the multifractal behavior of financial time series such that we have a Hurst exponent $[H(q)]$ that scales with the $q$th moment of the time series [43,44]. Furthermore, since the TFS is observed in cumulative time series with a fixed optimal window size [1,8,9], it is not possible to relate the TFS to the Hurst exponent that is defined with a moving time window [45]. Thus, if one considers that $T$ is calculated on time series of diffusive trajectory (which depend on the size of the time window), then it is possible to think that a more natural connection with the Hurst exponent could be defined through $T$. In that sense, it should be noted that the Hurst exponent ($H$) is a long-range memory measure in a time series such that if: (i) $H = 0.5$, then the current value of the time series does not depend on the previous values; (ii) $0 < H < 0.5$, then the value of the time series in the future tends to reverse the trend of the present; and (iii) $0.5 < H < 1$, then the value of the time series in the future tends to reinforce the trend of the present [45–49]. In addition, we hope to study the behavior of exponent $\beta$ in the future by Feynman path integral formalism to be able to establish more facts about TTS in complex systems. In fact, this idea, which goes beyond the scope of this paper, consists of studying the behavior over the time of the exponent $\beta$ of the TTS and the possible dependence between $\beta$ and the time variation of the Hurst exponent $H(t)$ using diffusive trajectory time series [50] and an integral definition of $T$ [25], which relates the probability density function of the underlying stochastic process obtained from the Feynman path integral formalism [9].

## ACKNOWLEDGMENTS

We acknowledge the support of the Physics Department of Universidad Nacional de Colombia. F.S.A. and C.J.Q. conceptualized the work; F.S.A. carried out the codes for the adjustments.

[1] Z. Eisler, I. Bartos, and J. Kertész, Adv. Phys. **57**, 89 (2008).
[2] A. Fronczak and P. Fronczak, Phys. Rev. E **81**, 066112 (2010).
[3] J. E. Cohen and M. Xu, Proc. Natl. Acad. Sci. USA **112**, 7749 (2015).
[4] S. H. Fairfield, J. Agric. Sci. **28**, 1 (1938).
[5] G. Blatter, M. V. Feigel'man, V. B. Geshkenbein, A. I. Larkin, and V. M. Vinokur, Rev. Mod. Phys. **66**, 1125 (1994).
[6] B. Mandelbrot, Intl. Econ. Rev. **1**, 79 (1960).
[7] M. Tokeshi, Res. Popul. Ecol. **37**, 43 (1995).
[8] Z. Eisler, J. Kertész, S. H. Yook, and A. L. Barabási, Europhys. Lett. **69**, 664 (2005).
[9] F. S. Abril and C. J. Quimbay, Phys. Rev. E **103**, 042126 (2021).
[10] P. Gopikrishnan, V. Plerou, L. A. Nunes Amaral, M. Meyer, and H. E. Stanley, Phys. Rev. E **60**, 5305 (1999).
[11] Z. Eisler and J. Kertész, Phys. Rev. E **73**, 046109 (2006).
[12] P. C. Ivanov, A. Yuen, and P. Perakakis, PLoS One **9**, e92885 (2014).
[13] C. Quimbay, Rev. Acad. Colomb. Cienc. Ex. Fis. Nat. **45**, 1039 (2021).
[14] N. Scafetta and P. Grigolini, Phys. Rev. E **66**, 036130 (2002).
[15] J. Johnston and H. Theil, Econ. J. **79**, 601 (1969).
[16] F. Bourguignon and C. Morrison, Am. Econ. Rev. **92**, 727 (2002).
[17] F. Bourguignon, Econometrica **47**, 901 (1979).
[18] L. Parker, Racial and Ethnic Segregation: In the News and On PolicyMap, https://www.policymap.com/2015/07/racial-and-ethnic-segregation-in-the-news-and-on-policymap/ (2015)
[19] A. F. Shorrocks, J. Econometrica **48**, 613 (1980).
[20] L. I. Kuncheva and C. J. Whittaker, Machine Learning **51**, 181 (2003).
[21] J. V. T. de Lima, J. M. de Araújo, and G. C. G. Z. dos Santos Lima, Eur. Phys. J. Plus **136**, 269 (2021).
[22] C. Gini, J. Political Econ. **87**, 769 (1997).
[23] I. Eliazar and I. M. Sokolov, Physica A **389**, 3023 (2010).
[24] J. María Sarabia, V. Jordá, and L. Remuzgo, Rev. Income Wealth **63**, 867 (2017).
[25] F. Cowell, *Theil, Inequality, and the Structure of Income Distribution* (Suntory and Toyota International Centres for Economics and Related Disciplines, London, UK, 2003).
[26] J. Miśkiewicz, Acta Phys. Pol. A **121**, B-89(2012).
[27] T. Andrei, B. Oancea, P. Richmond, D. Gurjeet, and H. Claudiu, Entropy **19**, 430(2017).
[28] J. Iglesias and R. de Almeida, Eur. Phys. J. B **85**, 85(2012).
[29] M. Salois, Physica A **392**, 2893 (2013).
[30] New York Times, Coronavirus (covid-19) data in the United States, https://github.com/nytimes/covid-19-data (2021)
[31] L. Blanco, V. Arunachalam, and S. Dharmaraja, *Introduction to Probability and Stochastic Processes with Applications*, 3rd ed., Vol. 1 (John Wiley & Sons, New York, NY, 2012).
[32] H. Kleinert, Physica A **311**, 536 (2002).
[33] H. Kleinert and X. J. Chen, Physica A **383**, 513 (2007).
[34] W. G. Cochran, Ann. Math. Statist. **23**, 315 (1952).
[35] L. Landau, Nature (London) **138**, 840 (1936).
[36] M. V. Milošević and R. Geurts, Physica C **470**, 791 (2010).

[37] M. E. Lines and A. M. Glass, *Principles and Applications of Ferroelectrics and Related Materials* (Clarendon Press, Oxford, UK, 1977).
[38] J. Als-Nielsen, *Phase Transitions and Critical Phenomena*, Vol. 5a (Academic Press, San Diego, CA, 1976), pp. 87–164.
[39] J. S. Rowlinson and F. L. Swinton, *Liquids and Liquid Mixtures: Butterworth's Monographs in Chemistry* (Butterworth Scientific, Oxford, UK, 1982), p. 437.
[40] R. K. Pathria and P. D. Beale, *Statistical Mechanics* (Elsevier, Amsterdam, 2011), p. 437.
[41] J. Chakravarty and D. Jain, J. Stat. Mech. (2021) 093204.
[42] C. E. Ekuma, G. C. Asomba, and C. M. I. Okoye, Physica C **472**, 1 (2012).
[43] T. D. Matteo, Quant. Finance **7**, 21 (2007).
[44] J. Barunik, T. Aste, T. D. Matteo, and R. Liu, Physica A **391**, 4234 (2012).
[45] L. A. Montoya, N. M. Aranda, and C. J. Quimbay, Physica A **421**, 124 (2015).
[46] H. E. Hurst, Trans. Am. Soc. Civil Eng. **116**, 770 (1951).
[47] A. G. Zawadowski, J. Kertész, and G. Andor, Physica A **344**, 221 (2004).
[48] J. Qi and H. Yang, Phys. Rev. E **84**, 066114 (2011).
[49] J. Kwapień, P. Oswięcimka, and S. Drożdż, Phys. Rev. E **92**, 052815 (2015).
[50] M. G. Tsionas, Physica A **567**, 125647(2021).